

Direct transition from a nematic phase to a polar biaxial smectic A phase in a homologous series of unsymmetrically substituted bent-core compounds†

R. Amaranatha Reddy and B. K. Sadashiva*

Raman Research Institute, C. V. Raman Avenue, Sadashivanagar, Bangalore, 560 080, India. E-mail: sadashiv@rri.res.in

Received 4th August 2003, Accepted 13th November 2003
First published as an Advance Article on the web 19th December 2003

The synthesis and characterization of twenty seven new compounds belonging to three homologous series of compounds derived from 3-hydroxybenzoic acid are reported. One of the terminal positions of the constituent molecules of these compounds is substituted with a strongly polar cyano group while the other end contains an *n*-alkyl chain attached to a biphenyl moiety. Twenty two of these compounds show the polar partial bilayer biaxial smectic A phase which is antiferroelectric in nature. In addition, a direct transition from the nematic phase to the polar partial bilayer biaxial smectic A phase which has not been seen before is also reported. The mesophases have been characterized using polarized light optical microscopy, differential scanning calorimetry, X-ray diffraction studies and electro-optical experiments.

Introduction

The theoretical prediction of the existence of the biaxial smectic A phase was made by de Gennes¹ nearly three decades ago. The biaxial smectic A phase has also been called the C_M phase (where M stands for McMillan) and Brand *et al.*,² have discussed theoretically its physical properties. However, the first experimental evidence for the occurrence of the biaxial smectic A phase was claimed in a binary mixture of liquid crystalline side chain polymer laterally substituted with naphthalene groups and a monomeric material.³ The binary phase diagram indicates that both the polymer and the monomer are completely miscible throughout the concentration range. Mixtures with up to 50 mol% of the monomeric liquid crystal show a nematic phase and the lower temperature phase has been claimed to be a biaxial smectic A phase. The biaxial smectic A phase has also been observed in a binary mixture of a metallomesogen and 2,4,7-trinitrofluorenone (TNF).⁴ In this case, the strong face to face interactions between TNF and the metallomesogen reduces molecular rotation around the long molecular axis, which leads to biaxiality. In addition, there is also a claim for the observation of a biaxial smectic A phase in a low molecular mass liquid crystalline material composed of boomerang-shaped molecules.⁵ The conoscopic experiments reveal the uniaxial interference pattern for the smectic A phase in the absence of an electric field. As pointed out by Hegmann *et al.*,⁴ in the above two cases^{3,5} the textural features of non-aligned samples resemble the uniaxial smectic A phase and unambiguous proof for the existence of the biaxial smectic A phase has not been provided.

The discovery⁶ of a electro-optically switchable mesophase in compounds composed of bent-core (BC) molecules, has opened a new sub-field of liquid crystals. Such compounds offer many exciting possibilities for new mesophases with interesting physical properties. Due to the specific shape of the molecules, unlike in calamitic liquid crystals, the in-layer properties can be varied (*m* is non-equivalent to $-m$) as shown

in Fig. 1. If the molecules are orthogonal with respect to the layer planes, the achiral mesophase is SmAP (polar smectic A) due to the polarization along the bent direction while in the chiral SmCP phase, the molecules are tilted. We examined some binary mixtures of a compound exhibiting the B_2 phase with one composed of rod-like molecules exhibiting the bilayer smectic A (SmA_2) phase which resulted in a very interesting phase diagram.^{7,8} At certain concentrations of the bent-core molecules (4–13 mol%), a biaxial smectic A_2 (SmA_{2b}) phase was induced in which the BC molecules underwent an orientational transition as the temperature was lowered from

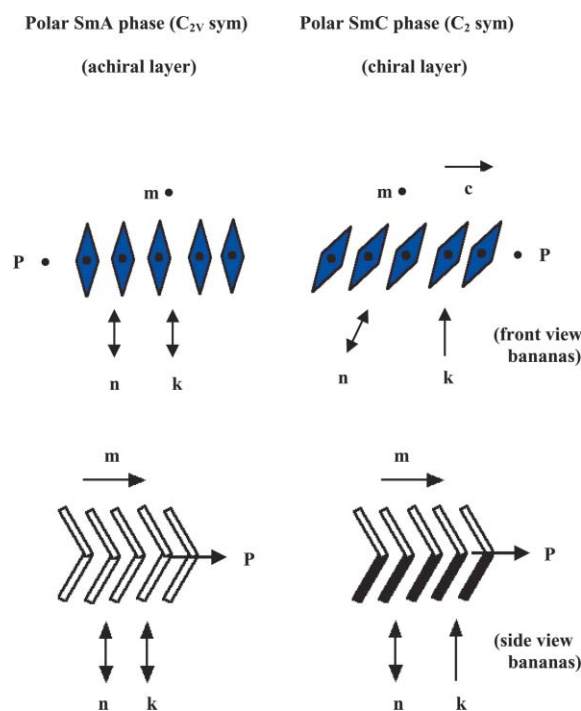


Fig. 1 A schematic representation of long molecular axis (*n*), layer normal (*k*), *c* vector (projection of *n*), in-plane director (*m*) and the in-layer polarization (*P*) for the chiral and achiral layers containing biaxial BC molecules which induce a polar packing within the layers resulting in a polarization along the bent direction.

† Electronic supplementary information (ESI) available: physical and spectral data obtained for the compounds of series **1j**, **1k** and **1l**. See <http://www.rsc.org/suppdata/jm/b3/b309262c/>

the uniaxial smectic A_2 phase. Perhaps, this represents the first experimental evidence for the existence of a biaxial smectic A phase in low molecular weight compounds, although in a mixture. Recently, we have reported^{9,10} the synthesis of several compounds composed of highly polar unsymmetrically substituted BC molecules which exhibit the partial bilayer biaxial smectic A (SmA_{db}) phase. All these compounds contain a highly polar cyano group at one terminal position of the constituent molecules which overlap in an antiparallel orientation. In fact, these compounds exhibit a direct transition from the uniaxial smectic A_d phase to a biaxial smectic A_d phase on lowering the temperature. We had reported that the SmA_{db} phase is apolar in both longitudinal and transverse directions. We now show that at fairly high electric fields and at high frequencies, the SmA_{db} phase is actually antiferroelectric in nature and it is designated as a SmA_dP_A phase. In view of the new experimental evidence, the quartet structure proposed earlier¹⁰ does not hold good. Here, we present the synthesis and characterization of three new homologous series of unsymmetrical compounds derived from 3-hydroxybenzoic acid. Many of these exhibit a direct transition from the nematic phase to the polar partial bilayer biaxial smectic A (SmA_dP_A) phase which represents the first example of such a transition in pure compounds. It is appropriate to mention here that recently Prehm *et al.*¹¹ have observed the biaxial smectic A phase in some rod-like bolaamphiphiles carrying a long semiperfluorinated chain. In addition, unambiguous experimental evidence for an achiral biaxial smectic A phase exhibiting an antiferroelectric switching behaviour has been provided by Eremin *et al.*¹²

The general molecular structure of the six-ring compounds under investigation is shown below. All the twenty seven compounds are esters and twenty two of them exhibit the SmA_dP_A phase.

Experimental

Materials

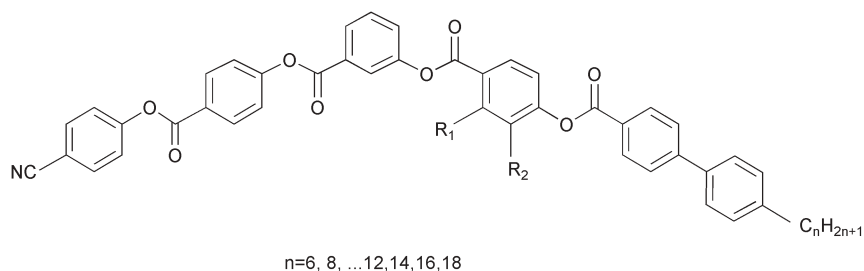
The unsymmetrically substituted strongly polar BC compounds belonging to the three different homologous series **Ij**, **Ik** and **Il** were synthesized following a procedure described earlier,¹⁰ except that in the final step, 4-*n*-alkylbiphenyl-4-carboxylic acids were used; the synthetic pathway is shown in Scheme 1. 3-Hydroxybenzoic acid and 4-cyanophenol were procured commercially and used without further purification. 2-Fluoro-4-hydroxybenzoic acid and 3-fluoro-4-hydroxybenzoic acid were prepared following procedures described in the literature.¹³ 4-Benzyloxybenzoic acid, 2-fluoro-4-benzyloxybenzoic acid and 3-fluoro-4-benzyloxybenzoic acid were synthesized following procedures described by us.¹⁴ The procedure for the

synthesis and characterization of compound **Ij10**, its spectral and analytical data are given below.

4-Cyanophenyl-4-{3-[4-(4-*n*-decylbiphenyl-4-carboxyloxy)benzoyloxy]benzoyloxy} benzoate, **Ij10**.

A mixture of 4-cyanophenyl-4-[3-(4-hydroxybenzoyloxy)benzoyloxy]benzoate¹⁰ (0.2 g, 0.42 mmol) and 4-*n*-decylbiphenyl-4-carboxylic acid (0.142 g, 0.42 mmol) was suspended in anhydrous chloroform (10 ml). To this reaction mixture was added *N,N*-dicyclohexylcarbodiimide, (0.1 g, 0.48 mmol) and a catalytic amount of 4-(*N,N*-dimethylamino)pyridine and the mixture was stirred at room temperature for 15 hours. The precipitated dicyclohexylurea was filtered off and chloroform (50 ml) was added to the filtrate. This organic solution was washed with 2% aqueous ice-cold sodium hydroxide solution (3×60 ml) and finally washed with water (4×75 ml) and dried over anhydrous sodium sulfate. The residue obtained after removal of solvent was chromatographed on silica gel using chloroform as an eluent. Removal of solvent from the eluate afforded a white material which was crystallized from butan-2-one, yield 58%; mp 169 °C; ¹H NMR (CDCl₃, 400 MHz) δ (ppm): 8.27–8.03 (m, 7H, Ar-H), 7.7–7.48 (m, 9H, Ar-H), 7.38–7.19 (m, 8H, Ar-H), 2.62–2.58 (t, ³J 7.68 Hz, 2H, Ar-CH₂-), 1.59–1.57 (quintet, ³J 6.86 Hz, 2H, Ar-CH₂-CH₂-), 1.57–1.21 (m, 14H, 7 \times -CH₂-), 0.83–0.8 (t, ³J 6.68 Hz, 3H, 1 \times -CH₃); IR (KBr) ν_{max} : 2922, 2852, 2243, 1736, 1605, 1275, 1080 cm⁻¹; C₅₁H₄₅NO₈ requires, C, 76.58; H, 5.67; N, 1.75%; found: C, 76.68; H, 5.56; N, 1.73%.

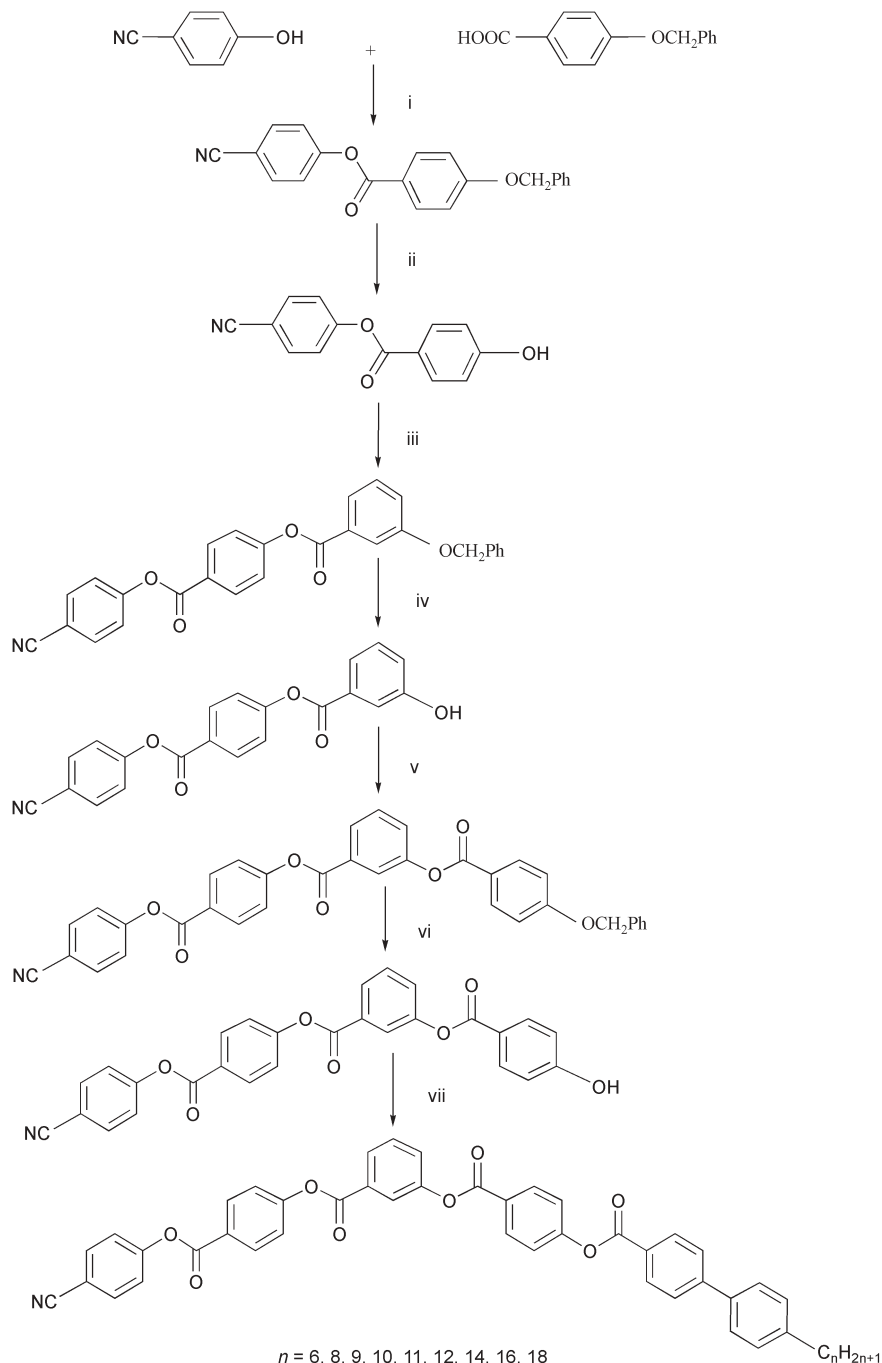
In general, the chemical structure of all the compounds was confirmed by ¹H NMR spectroscopy (Bruker AMX400 spectrometer) with 1% tetramethylsilane in deuteriochloroform as an internal standard, infrared spectral data (Shimadzu FTIR-8400 spectrophotometer) and elemental analysis (Carlo-Erba 1106 analyzer). The thermal behaviour was investigated using a polarized light optical microscope (Leitz Laborlux 12 POL/Olympus BX 50) equipped with a heating stage and a controller (Mettler FP52 and FP5 respectively) and also from thermograms recorded on a differential scanning calorimeter (Perkin-Elmer Model, Pyris 1D). The enthalpy values of various transitions were also determined using the latter method. The calorimeter was calibrated using pure indium as a standard. X-Ray diffraction measurements on non-oriented samples were carried out using Cu-K α radiation from a rotating anode generator (Rigaku Ultrax 18) with a flat graphite crystal monochromator. The diffraction patterns were recorded on an image plate (Marresearch). The samples were taken in Lindemann capillaries and the sample temperature in each case was controlled to within ± 0.1 °C. The conoscopic experiments and birefringence measurements were carried out using a microscope (Leitz Ortholux – II POL BK) equipped with a



$R_1=H, R_2=H$ Series-**Ij**

$R_1=F, R_2=H$ Series-**Ik**

$R_1=H, R_2=F$ Series-**Il**



Scheme 1 General synthetic pathway used for the preparation of unsymmetrically substituted banana-shaped mesogens. *Reagents and conditions:* (i) DCC, cat. DMAP, dry CHCl_3 , room temp., 15 h, 81%; (ii) cat 5% Pd-C, H_2 , 1,4-dioxane, 55 °C, 75%; (iii) 3-benzyloxybenzoic acid, DCC, cat. DMAP, dry CHCl_3 , room temp., 15 h, 72%; (iv) cat 5% Pd-C, H_2 , 1,4-dioxane, 55 °C, 73%; (v) 4-benzyloxybenzoic acid, DCC, cat. DMAP, dry CHCl_3 , room temp., 20 h, 68%; (vi) cat. 5% Pd-C, H_2 , 1,4-dioxane, 55 °C, 80%; (vii) 4-*n*-alkylbiphenyl-4-carboxylic acids, DCC, cat. DMAP, dry CHCl_3 , room temp., 15 h, 50–60%.

heating stage and a controller (Mettler FP 82 and FP 80HT respectively).

Results and discussion

The phase transition temperatures and the associated enthalpy values for the 27 highly polar unsymmetrically substituted compounds belonging to the three different homologous series **1j**, **1k** and **1l** are summarized in Tables 1, 2 and 3 respectively. All nine compounds of the **1j** series are mesomorphic. On slow cooling a thin film of the isotropic liquid of compound **1j6** under a polarizing microscope, birefringent droplets appear which vanish subsequently to give rise to a homeotropic texture. However, in some regions of the slide 2- and 4-brush

defects, which are the characteristic features of the uniaxial nematic phase could be seen. Similar textural features could also be seen for compounds **1j8** to **1j11** indicating a uniaxial nematic phase. The clearing transition enthalpy value for this phase is in the range of 0.4 to 0.6 kJ mol^{-1} . Compounds **1j8** and **1j9** show an additional monotropic phase. On slow cooling a homeotropically aligned nematic phase of compound **1j9**, a schlieren texture with 2- and 4-brush defects were obtained indicating the biaxiality of the lower temperature phase. The presence of the 2-brush defects in the lower temperature phase indicates that the mesophase is polar and is also a distinguishing feature of the biaxial smectic A_d phase.¹⁰ This mesophase shows an antiferroelectric switching behaviour, which will be described later. The sample was also

Table 1 Transition temperatures (°C) and enthalpies (kJ mol⁻¹) for compounds of series **1j**^a

Compound	<i>n</i>	Cr	SmA _d P _A	SmA _d	N	I			
1j6	6	·	156.0 46.7	—	—	·	204.0 0.48		
1j8	8	·	170.0 50.2	·	(151.5) ^b	—	·	195.0 0.45	
1j9	9	·	160.0 39.2	·	(158.0)	—	·	189.8 0.43	
1j10	10	·	169.0 56.8	·	171.3 0.15	·	174.8 0.2	·	189.0 0.47
1j11	11	·	169.0 44.7	·	176.5 0.13	·	185.3 0.4	·	187.5 0.57
1j12	12	·	158.0 53.6	·	181.0 0.25	·	192.0 2.9	—	·
1j14	14	·	157.0 58.5	·	184.3 0.16	·	199.2 4.76	—	·
1j16	16	·	156.0 38.4	·	185.0 0.1	·	204.5 5.8	—	·
1j18	18	·	154.0 65.4	·	184.0 0.09	·	206.7 6.6	—	·

^a key for all three Tables 1–3: Cr:crystalline phase; SmA_d:partial bilayer uniaxial smectic A phase; SmA_dP_A:partial bilayer biaxial antiferroelectric smectic A phase; SmX:unidentified antiferroelectric smectic phase; N:nematic phase; I:isotropic phase. · phase exists; — phase does not exist; temperature in parentheses indicate monotropic transitions. ^b enthalpy could not be determined as the sample crystallizes immediately.

Table 2 Transition temperatures (°C) and enthalpies (kJ mol⁻¹) for compounds of series **1k**

Compound	<i>n</i>	Cr	SmA _d P _A	SmA _d	N	I			
1k6	6	·	175.5 57.8	—	—	·	197.2 0.42		
1k8	8	·	155.0 53.1	—	—	·	184.9 0.4		
1k9	9	·	160.0 52.3	·	(152.5)	—	·	183.0 0.4	
1k10	10	·	161.5 48.2	·	162.5 0.2	·	166.0 0.1	·	179.8 0.38
1k11	11	·	161.5 58.9	·	168.0 0.18	·	177.0 0.3	·	180.2 0.57
1k12	12	·	160.0 45.6	·	172.5 0.1	·	183.0 2.7	—	·
1k14	14	·	159.5 42.8	·	176.8 0.14	·	191.0 4.54	—	·
1k16	16	·	158.0 48.9	·	178.2 0.06	·	197.0 5.8	—	·
1k18	18	·	157.5 49.9	·	179.2 0.05	·	202.0 6.6	—	·

examined in a homogeneously aligned cell. A photomicrograph showing the transition from the nematic phase to the polar biaxial smectic A_d phase and the texture of the polar biaxial

smectic A_d phase are shown in Fig. 2. A fan-shaped texture with sharp lines over the fans excludes the possibility of a SmC phase which normally exhibits a broken fan-shaped texture. As

Table 3 Transition temperatures (°C) and enthalpies (kJ mol⁻¹) for compounds of series **1l**

Compound	<i>n</i>	Cr	SmX	SmA _d P _A	SmA _d	N	I				
1l6	6	·	159.5 54.0	—	—	—	·	197.5 0.59			
1l8	8	·	157.0 40.2	—	—	—	·	186.4 0.47			
1l9	9	·	154.0 35.9	—	·	(149.0)	—	·	183.1 0.35		
1l10	10	·	158.0 40.2	—	·	162.0 0.13	·	166.9 0.1	·	179.8 0.69	
1l11	11	·	158.0 37.4	—	·	167.0 0.13	·	177.6 0.48	·	179.8 0.58	
1l12	12	·	154.5 38.7	—	·	170.3 0.11	·	182.0 3.15	—	·	
1l14	14	·	153.0 43.4	—	·	174.0 0.1	·	189.5 4.8	—	·	
1l16	16	·	148.5 47.0	·	160.0 0.34	·	176.2 0.17	·	195.0 5.8	—	·
1l18	18	·	149.0 44.5	·	166.0 0.1	·	176.5 0.12	·	199.5 6.36	—	·

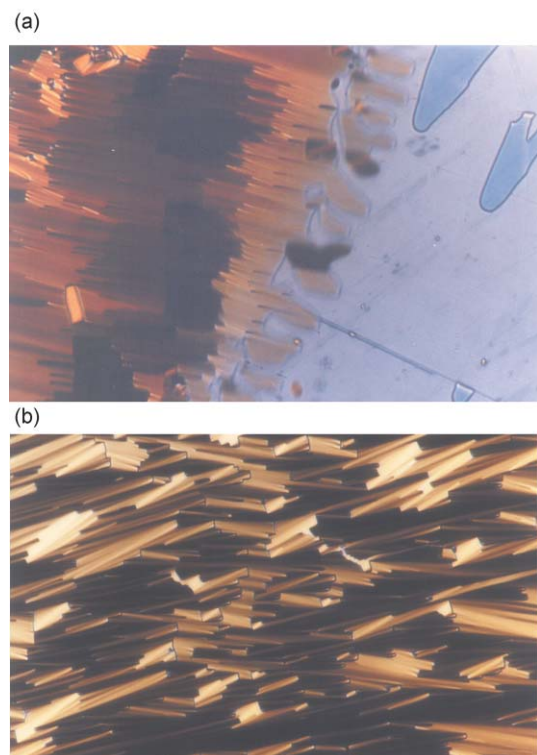


Fig. 2 Photomicrographs showing (a) a transition from a nematic phase to a polar biaxial smectic A_d phase and (b) a texture of the polar biaxial smectic A_d phase obtained in a homogeneously aligned cell for compound **1j9**.

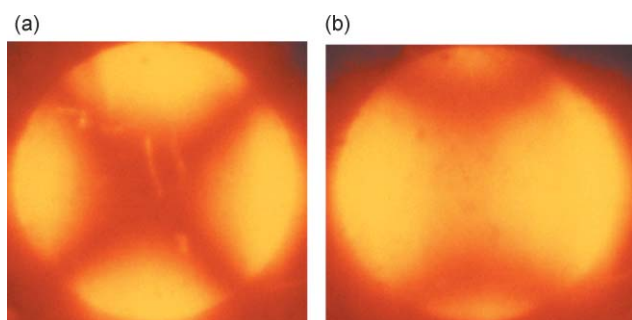


Fig. 3 Photomicrographs of the conoscopic patterns obtained from a homeotropically aligned sample of compound **1j9**: (i) a uniaxial pattern in the nematic phase at 162 °C, and (ii) a biaxial pattern in the SmA_dP_A phase at 156 °C.

we shall see later, the XRD measurements indicate that the lower temperature phase of compound **1j9** has a partial bilayer structure. The confirmation of the existence of the biaxial smectic A_d phase was obtained by conoscopic experiments. The uniaxial interference pattern in the nematic phase splits as the temperature is lowered and the patterns obtained in the two phases are shown in Fig. 3. On lowering the temperature slightly (*e.g.* 0.2 °C) the isogyres move away from the field of view. These observations clearly indicate that the lower temperature phase is in fact a polar biaxial smectic A_d phase. The enthalpy value of this transition is in the range of 0.2 to 0.5 kJ mol⁻¹. Perhaps, this is the first example of a compound showing a direct transition from the uniaxial nematic phase to a polar partial bilayer biaxial smectic A (SmA_dP_A) phase. It has been predicted theoretically¹⁶ that, if the lower temperature SmA phase is biaxial then the high temperature nematic phase is supposed to be biaxial. Contrary to this, we observe only a uniaxial nematic to a biaxial SmA phase transition.

On ascending the homologous series, the polar biaxial smectic A_d phase gets stabilized and the uniaxial smectic A_d

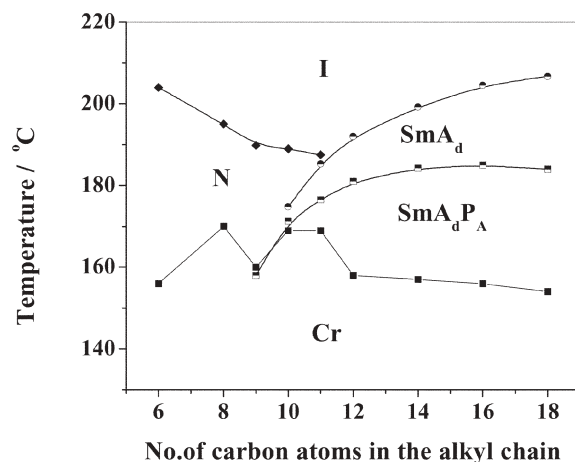


Fig. 4 Plot of the transition temperatures as a function of the number of carbon atoms in the n -alkyl chain for homologues of series **1j**.

phase is induced, and these two phases exist even for a compound (**1j18**) with an n -octadecyl chain. While compounds **1j10** and **1j11** are trimesomorphic, on ascending the homologous series, the uniaxial nematic phase gets eliminated. It is also interesting to note that the thermal range of the SmA_dP_A phase increases from 2.3° for compound **1j10** to 30 °C for compound **1j18** on ascending the series. A plot of the transition temperatures as a function of the terminal n -alkyl chain for series **1j** is shown in Fig. 4.

As can be seen in Table 2, the lower homologues of series **1k** *viz.* compounds **1k6** and **1k8** exhibit only a uniaxial nematic phase, while compound **1k9** shows a direct transition from the nematic phase to a polar biaxial smectic A_d phase. Compounds **1k10** and **1k11** show nematic, uniaxial smectic A_d and polar biaxial smectic A_d phases on cooling the isotropic phase. However, as observed in series **1j**, the higher homologues (**1k12**, **1k14**, **1k16** and **1k18**) exhibit SmA_d and SmA_dP_A phases. The textural features of the three mesophases of this series of compounds are similar to those obtained for the compounds of series **1j**. The conoscopic patterns obtained in the uniaxial and biaxial smectic A_d phases for compound **1k12** are shown in Fig. 5. In this series also only two homologues are trimesomorphic and the thermal range of the SmA_dP_A phase increases on increasing the terminal chain length. The introduction of a fluorine substituent *ortho* to the carbonyl group suppresses the clearing temperatures while the melting point increases for most of the homologues. A plot of the transition temperatures as a function of the terminal n -alkyl chain length for series **1k** is shown in Fig. 6 and one can see that the like transition points fall on smooth curves.

In the case of compounds of series **1l** whose transition

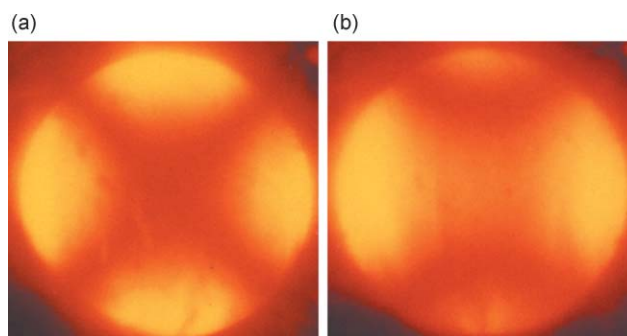


Fig. 5 Photomicrographs of the conoscopic patterns obtained for a homeotropically aligned sample of compound **1k12**, (i) the uniaxial smectic A_d phase at 175 °C, and (ii) the polar biaxial smectic A_d phase at 171 °C.

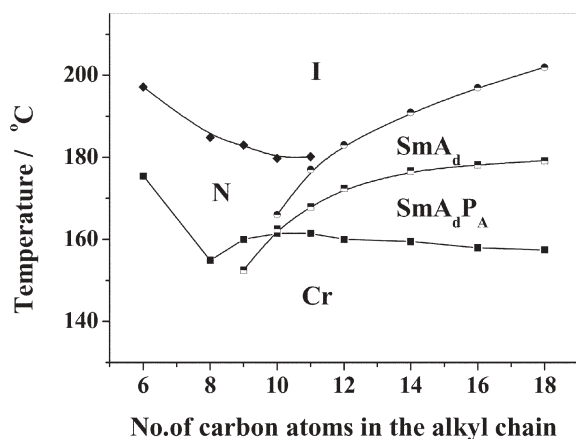


Fig. 6 Plot of the transition temperatures as a function of the number of carbon atoms in the *n*-alkyl chain for homologues of series **1k**.

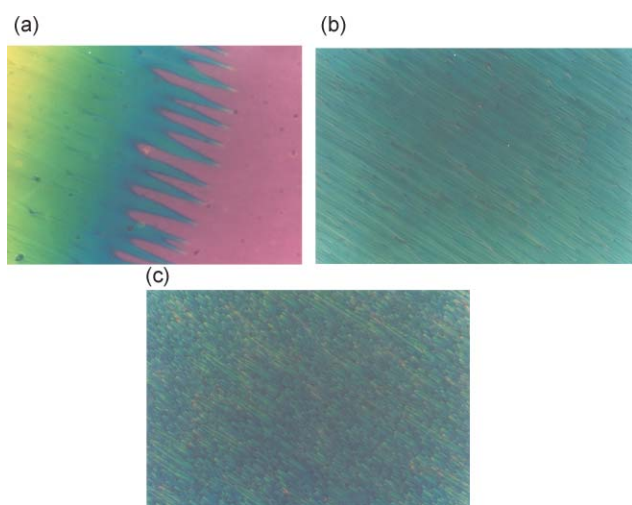


Fig. 7 Photomicrographs of the texture showing (a) a transition from a nematic phase to a uniaxial smectic A_d phase, (b) a uniaxial smectic A_d phase and (c) a polar biaxial smectic A_d phase in a homogeneously aligned cell of a sample of compound **1111**.

temperatures and associated enthalpy values are given in Table 3, the mesomorphic behaviour is similar to that observed for series **1j** and **1k** except that compounds **1116** and **1118** show an additional mesophase below the SmA_dP_A phase.

A photomicrograph showing a phase transition from the uniaxial nematic phase to the SmA_d phase for compound **1111** is shown in Fig. 7(a). Photomicrographs of the textures observed for the fully formed SmA_d and SmA_dP_A phases for the same compound are shown in Fig. 7(b) and Fig. 7(c) respectively. A schlieren texture is obtained when the homeotropically aligned SmA_d phase is cooled to the SmA_dP_A phase and a typical texture observed for compound **1111** is shown in Fig. 8. Interestingly, compounds **1116** and **1118** show trimesomorphism and the lowest temperature phase was not observed in series **1j** and **1k**. On slow cooling a sample of the homeotropically aligned SmA_d phase of compound **1116** to a temperature of 175 °C, a schlieren texture with both 2- and 4-brush defects could be obtained indicating that the phase is a polar biaxial smectic A_d phase as observed for the lower homologues **119** to **1114**. A photomicrograph of the texture obtained for the SmA_dP_A phase of compound **1116** is shown in Fig. 9(a). On cooling this SmA_dP_A phase to a temperature of 160 °C, a transition takes place and a further decrease in the temperature increases the birefringence of the mesophase and a photomicrograph of this texture is shown in Fig. 9(b). Similar mesomorphic behaviour was observed for compound **1118** also. The enthalpy of this transition is of the order of 0.1 to

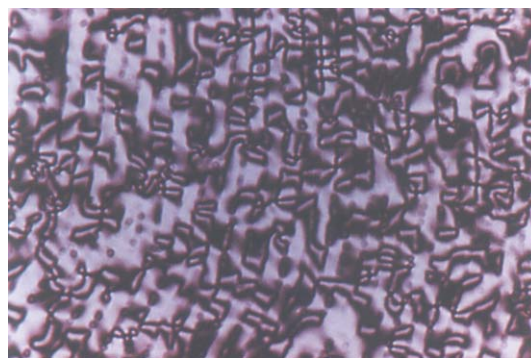


Fig. 8 Photomicrograph of a schlieren texture obtained in the polar biaxial smectic A_d phase exhibited by compound **1111** at 160 °C.

0.3 kJ mol⁻¹. The 2- and 4-brush defects observed in the higher temperature SmA_dP_A phase is retained in this lower temperature phase also. This mesophase has been designated as SmX phase since its structure is not clearly understood. In series **11**, only one compound, **119** showed a direct transition from the uniaxial N phase to the SmA_dP_A phase though the latter is monotropic. The enthalpy value obtained for the SmA_d-N phase transition varied from 0.1 to 0.48 kJ mol⁻¹ and for the SmA_d-I phase transition, it was 3.15 to 6.36 kJ mol⁻¹. However, for the SmA_dP_A phase to SmA_d phase transition, the enthalpy value was fairly low and was of the order of 0.1 to 0.23 kJ mol⁻¹. A plot of the transition temperatures versus the number of carbon atoms in the *n*-alkyl chain for the homologues of series **11** is shown in Fig. 10.

XRD experiments were performed following a procedure described previously.^{9,10} Eight different compounds belonging to the three homologous series were examined. The non-oriented samples, in the smectic phase showed a sharp reflection in the small angle region corresponding to the layer spacing. The second order reflection obtained was found to be somewhat weak. In addition, a diffuse wide-angle

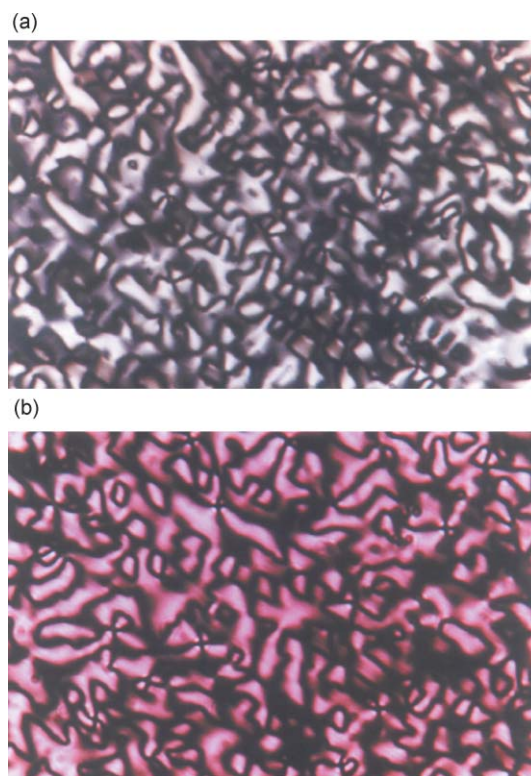


Fig. 9 Photomicrographs obtained for compound **1116**, (a) schlieren texture in the SmA_dP_A phase and (b) more birefringent schlieren texture in the SmX phase.

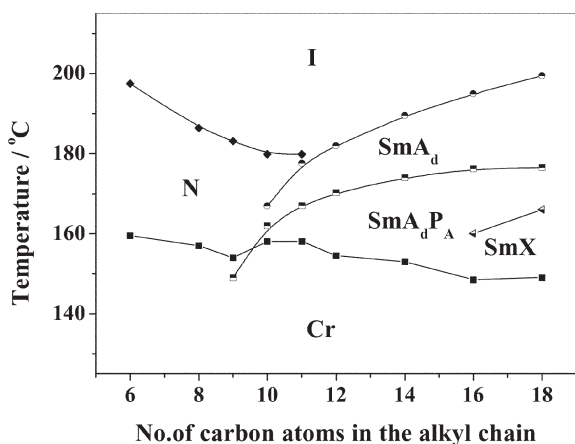


Fig. 10 Plot of the transition temperatures as a function of the number of carbon atoms in the *n*-alkyl chain for homologues of series 11.

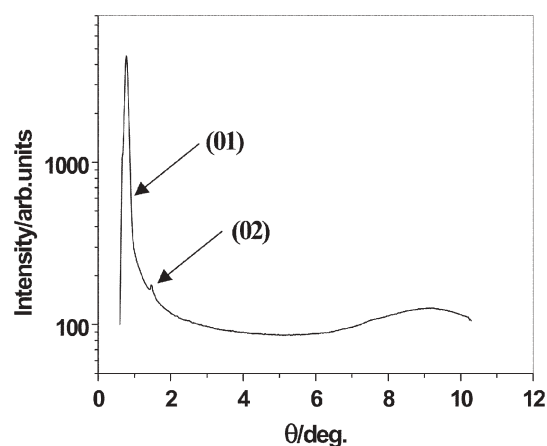


Fig. 11 Intensity profile of the X-ray diffraction pattern in the SmA_dP_A phase of compound **1116** obtained at 166°C as a function of the Bragg angle θ .

scattering with a maximum at 4.7 \AA was obtained indicating a liquid-like in-plane order. As described earlier,^{9,10} the layer spacing, d was found to be temperature independent in both the smectic phases. The X-ray angular intensity profile obtained in the SmA_dP_A phase of compound **1116** is shown in Fig. 11. The layer spacings d , obtained from XRD studies, for the smectic phases of eight compounds investigated and the calculated molecular length L in the most extended form with an all *trans* conformation of the *n*-alkyl chain are given in Table 4. It can be seen that the layer spacing d , is significantly larger than the calculated molecular length. This provides evidence for a partial bilayer structure of the smectic layers, in both the higher and lower temperature mesophases. No change in the layer

Table 4 The layer spacings d obtained from XRD studies, for the smectic phases of several compounds investigated and the molecular length L , measured in the most extended form with an all *trans* conformation of the chain

Compound	$d/\text{\AA}$		$L/\text{\AA}$
	First order	Second order	
1j9	48.6	24.3	43.3
1j11	51.3	—	45.4
1j16	58.8	29.4	51.1
1k11	52.0	—	45.4
1k16	57.8	28.9	51.1
1111	54.4	—	45.4
1116	58.8	29.4	51.1
1118	61.7	30.8	53.5

spacing could be observed from X-ray experiments, while cooling the SmA_dP_A to the SmX phase obtained for compounds **1116** and **1118**. Interestingly, both these mesophases switch electro-optically and hence we have designated them as SmA_dP_A and SmX phases respectively. A space filling model of an antiparallel arrangement of strongly polar molecules used to measure the length of the partial bilayer structure is shown in Fig. 12. Similar molecular conformations have been considered by Eremin *et al.*¹² and Schroder *et al.*¹⁵ for the polar biaxial smectic A phases in compounds containing two terminal chains. However, in the system studied by us, the molecules contain a strongly polar terminal cyano group which facilitates an antiparallel arrangement of the molecules resulting in a partial bilayer structure. For example, a compound containing an *n*-undecyl chain would give a value of 57 \AA (1, as shown in Fig. 12). As can be seen in Table 4, we found a value of 54.4 \AA for compound **1111**. Since there can be interlayer interactions (and/or *gauche* conformation of chains), the experimentally observed values are slightly lower.

Electro-optical switching behaviour has been examined for several compounds of the three homologous series of compounds. As an example, the switching behaviour of compound **1118** is described here. A cell having a thickness of $18\text{ }\mu\text{m}$ was constructed for aligning the sample homogeneously. The isotropic liquid of this compound was cooled slowly under a triangular-wave electric field of about $\pm 280\text{ V}$ at a frequency of 1 kHz until the smectic A_d phase was obtained. No polarization current peak/s could be observed in this high temperature uniaxial smectic A_d phase. However, on cooling the sample to a temperature of about 174°C (the temperature was found to decrease by about 2° due to the dissipation caused by ion flow), two polarization current peaks slowly appeared for each half period indicating an antiferroelectric ground state structure for the lower temperature biaxial smectic A_d phase. The electro-optical current response trace obtained in this phase is shown in Fig. 13. The current was measured across $1\text{ k}\Omega$ resistance

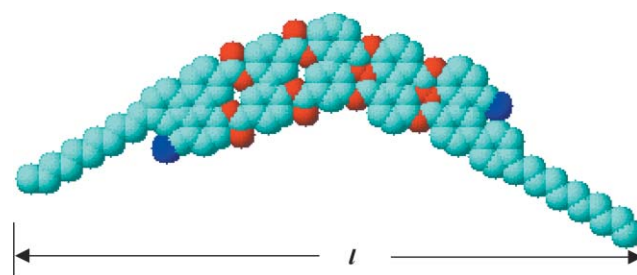


Fig. 12 A space filling model of the antiparallel arrangement of strongly polar molecules used to measure the length of the partial bilayer structure.

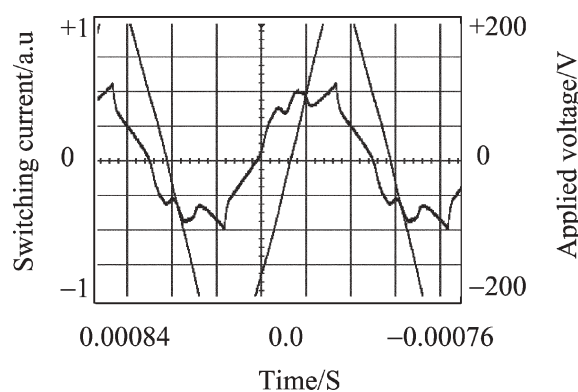


Fig. 13 Switching current response trace obtained by applying a triangular-wave voltage of about $\pm 280\text{ V}$ at 1 kHz in the SmA_dP_A phase of compound **1118** at 170°C ; polarization value $P \approx 140\text{ nC cm}^{-2}$; cell thickness, $18\text{ }\mu\text{m}$.

and the polarization value determined is about 140 nC cm^{-2} . No optical switching could be observed due to the absence of layer chirality and only a focal-conic texture was observed which was also independent of the polarity of the applied field.¹² The additional sharp lines obtained in the focal-conic texture of the SmA_dP_A phase disappeared on application of an electric field. On turning off the electric field, no striped pattern along the smectic layers could be seen indicating the absence of the tilt of the BC molecules. If the molecules were to be tilted in the mesophase, then we should have seen optical switching as observed for the B_2 phase. In addition, we do see strong dynamic fluctuations in this phase as observed by Eremin *et al.*¹² and Schroder *et al.*¹⁵ and such fluctuations are not seen in the tilted smectic phases. This supports the orthogonal arrangement of molecules in the mesophase. On lowering the temperature further into the SmX phase, the two polarization current peaks were retained indicating the antiferroelectric nature of the mesophase but the saturated polarization value increased to 250 nC cm^{-2} . A trace of the current response obtained in this SmX phase is shown in Fig. 14. However, from the available data, it is difficult to speculate the exact nature of the lower temperature SmX phase. An increase in the birefringence and also the polarization value, suggests a tilt of the molecules in this mesophase, which cannot be detected from XRD studies. As pointed out by Brand *et al.*,¹⁶ SmA phase to SmC phase transition can be divided into two steps. First there could be a smectic A to C_M phase transition during which a preferred direction in the layers arise, which still could maintain the orthogonal arrangement of the molecules. In the second step, during the C_M to smectic C phase transition, a tilt arises leading to the biaxiality in the tilted SmC phase.

It is necessary for us to point out the following concerning the biaxial smectic A_d phase. We had reported¹⁰ earlier, that the partial bilayer biaxial smectic A phase is apolar in both longitudinal and transverse directions and had proposed a quartet structure for the arrangement of these highly polar unsymmetrical bent-core molecules. In the light of null transmission ellipsometry experiments¹⁹ on one of the compounds *viz.* **1g14** studied earlier, and also electro-optical experiments described below for another homologue (**1g16**), the proposed quartet structure is not applicable to these systems. The switching behaviour of the mesophases of compound **1g16** was re-examined as follows. On cooling the isotropic liquid of this compound in a homogeneously aligned cell (cell thickness, $9.4 \mu\text{m}$), under a triangular-wave electric field of about $\pm 150 \text{ V}$ and a frequency of 500 Hz , a focal-conic texture was obtained. No polarization current peak/s could be observed in this higher temperature SmA_d phase. On lowering the temperature, a phase transition occurred to a SmA_{db} phase (according to the earlier nomenclature) and the growth of two polarization current peaks for each half period could be clearly

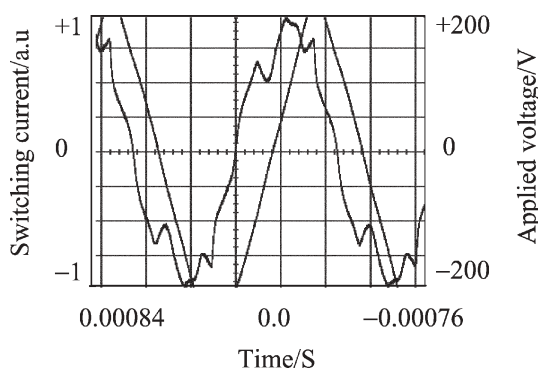


Fig. 14 Switching current response obtained by applying a triangular-wave voltage of about $\pm 280 \text{ V}$ at 1 kHz in the SmX phase of compound **1118** at $152 \text{ }^\circ\text{C}$; polarization value $P \approx 250 \text{ nC cm}^{-2}$; cell thickness, $18 \mu\text{m}$.

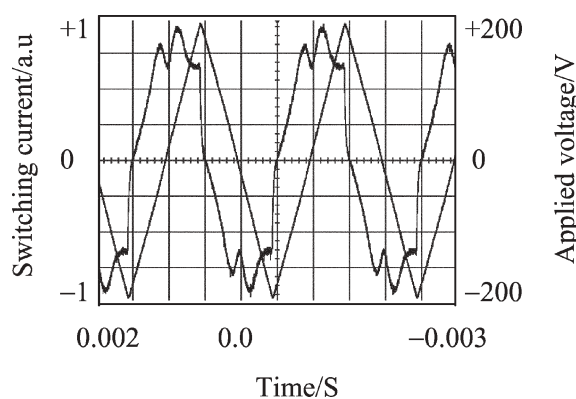


Fig. 15 Switching current response obtained in the SmA_dP_A phase at $132 \text{ }^\circ\text{C}$ exhibited by compound **1g16** by applying a triangular-wave voltage $\pm 190 \text{ V}$ at 500 Hz (threshold $\pm 125 \text{ V}$); polarization value, $P \approx 125 \text{ nC cm}^{-2}$; cell thickness, $9.4 \mu\text{m}$.

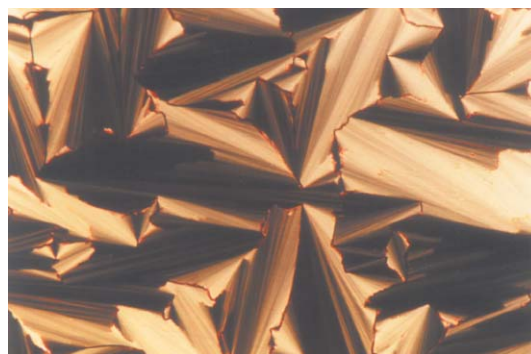


Fig. 16 Optical photomicrograph obtained under the same conditions given in Fig. 15 for the same compound.

seen. The current was measured across $1 \text{ k}\Omega$ resistance. The saturated polarization value calculated at $\pm 190 \text{ V}$ (threshold, $\pm 125 \text{ V}$ at 500 Hz) is about 125 nC cm^{-2} . The electro-optical response trace obtained is shown in Fig. 15. The optical photomicrograph obtained under these conditions is shown in Fig. 16. These experimental observations reveal that the molecular bow plane is orthogonal to the layer planes and the polarization is antiparallel in adjacent layers. It is likely that the molecules form a polar non-tilted smectic layer which is due to the strong anisotropic interactions caused by the very specific shape of the molecules. The energetically more probable structure is antiferroelectric ordering of the dipoles in adjacent layers which agree well with the observed optical textures, which show both 2- and 4-brush defects. The 2-brush defects in this case are dispirations,^{17,18} which are combinations of half strength disclinations which are defect patterns in the in-plane director, and screw dislocations. We have given a fairly detailed account of these in our earlier studies^{9,10} on two other similar systems. Based on these experimental observations, a molecular model has been proposed for the SmA_dP_A phase and is shown in Fig. 17. It should be mentioned here that though we had considered this model earlier, it was ruled out based on the observations made under those experimental conditions. The above model is similar to the one proposed by Eremin *et al.*¹² for a polar biaxial smectic A phase.

We have also carried out quantitative measurements of the in-layer birefringence ($\Delta\mu$) in the SmA_dP_A and SmX phases of compound **1118** using a quarter wave plate as a compensator at $\lambda 5893 \text{ \AA}$. For this purpose, well aligned samples were obtained as follows. A cell was constructed in which one of the plates is conducting (ITO coated) having a gap of $85 \mu\text{m}$ that is etched out. The other plate is an ordinary glass slide and both of them are pretreated with octadecyltriethoxysilane (ODSE) for obtaining the homeotropic alignment. The cell thickness was

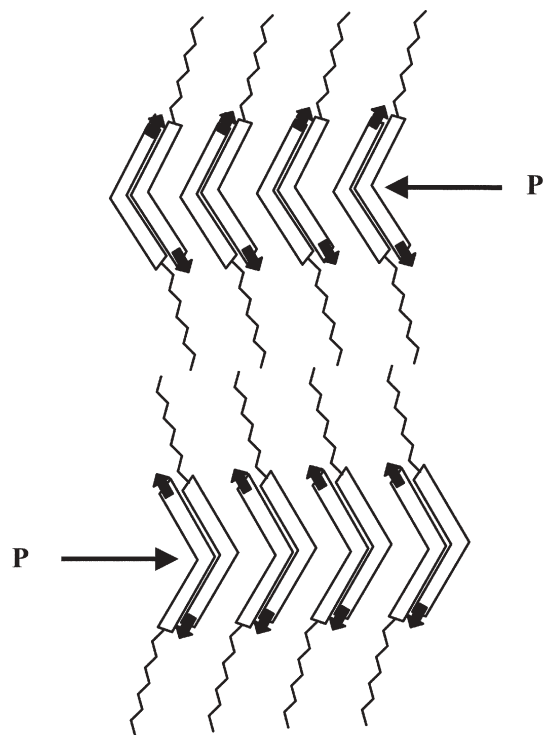


Fig. 17 A schematic representation of a polar packing of molecular pairs within the layer with an antiferroelectric ordering between successive layers.

adjusted to be $37.3 \mu\text{m}$ using appropriate spacers. The oven temperature was maintained to an accuracy of about 5 mK . A square-wave electric field of about $0.68 \text{ V } \mu\text{m}^{-1}$ at a frequency of 10 kHz was applied between the electrodes to obtain an aligned sample. The optical measurements were carried out under a continuous application of electric field by slow cooling the sample from the uniaxial to the biaxial smectic A_d phase (T_{ub}) and to the SmX phase until the sample crystallizes. A plot of in-layer birefringence ($\Delta\mu$) as a function of temperature ($T_{ub} - T$) is shown in Fig. 18. The in-layer birefringence continuously increases on lowering the temperature in the SmA_dP_A and SmX phases. This value increases from 0.007 (at T_{ub} transition) to 0.011 in the SmA_dP_A phase and from 0.0114 to 0.02 in the SmX phase. Though the DSC thermogram shows a weakly first order phase transition, no significant jump in the in-layer birefringence could be observed at the transition

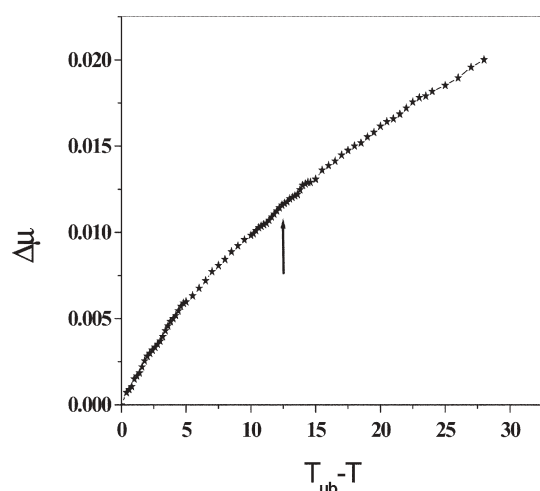


Fig. 18 A plot of in-layer birefringence ($\Delta\mu$) as a function of temperature ($T_{ub} - T$) in the SmA_dP_A and SmX phases of compound **1118**. The arrow shows the transition point from SmA_dP_A to SmX phase.

from the SmA_dP_A to the SmX phase. However, this cannot rule out the possibility of the tilt of BC molecules with respect to the layer normal which coincides with optic axis in this arrangement. Perhaps, the local heating problem of the sample by the continuous application of electric field has an influence on the measured values.

Some general observations can be made concerning the mesomorphic properties of these three homologous series of compounds. The introduction of fluorine at *ortho* position (series **1k**) reduces the clearing temperatures by about $10 \text{ }^\circ\text{C}$ while the melting points are increased marginally. The mesophase thermal ranges of both the SmA_d and SmA_dP_A phases are reduced as a result of *ortho*-fluoro substitution. However, in the case of *meta*-fluorine substituted compounds (series **1l**), both melting as well as clearing temperatures are reduced by about $5\text{--}10 \text{ }^\circ\text{C}$. Also, an additional unidentified antiferroelectric SmX phase has been observed for higher homologues. The clearing temperature is highest for $n = 18$ in all three series of compounds. This is in complete contrast to what is normally observed for the SmA phase in a homologous series of calamitic liquid crystals where this temperature decreases on ascending a series. A cursory look at the plots shown in Fig. 4, 6 and 10 clearly shows that the clearing temperature curve for the SmA_d phase rises and goes above the falling $N \rightarrow I$ curve. This is again unusual and not observed in calamitic liquid crystals.

Conclusions

Three new homologous series of unsymmetrically substituted compounds composed of bent-core molecules containing a highly polar cyano terminal substituent have been synthesized. XRD studies show that the both the smectic A phases have partial bilayer structure as also the unidentified SmX phase. The lower temperature partial bilayer biaxial smectic A phase and the SmX phases are antiferroelectric in nature. A model has been proposed for the polar packing of molecular pairs within the layer with an antiferroelectric ordering between successive layers. Out of the 27 compounds investigated, 22 show the partial bilayer polar biaxial smectic A (SmA_dP_A) phase and 4 of them show a direct transition from the nematic phase, which has been observed for the first time.

Acknowledgements

The authors thank Ms K. N. Vasudha for technical support and the Sophisticated Instruments Facility, Indian Institute of Science, Bangalore for recording the NMR spectra.

References

- 1 P. G. de Gennes, *The Physics of Liquid Crystals*, Clarendon, Oxford, 1974, p. 279.
- 2 H. R. Brand, P. E. Cladis and H. Pleiner, *Macromolecules*, 1992, **25**, 7223.
- 3 H. F. Leube and H. Finkelmann, *Makromol. Chem.*, 1991, **192**, 1317.
- 4 T. Hegmann, J. Kain, S. Diele, G. Pelzl and C. Tschierske, *Angew. Chem., Int. Ed.*, 2001, **40**, 887.
- 5 K. J. K. Semmler, T. J. Dingemans and E. T. Samulski, *Liq. Cryst.*, 1998, **24**, 799.
- 6 T. Niori, J. Sekine, J. Watanabe, T. Furukawa and H. Takezoe, *J. Mater. Chem.*, 1996, **6**, 1231.
- 7 R. Pratibha, N. V. Madhusudana and B. K. Sadashiva, *Science*, 2000, **288**, 2184.
- 8 R. Pratibha, N. V. Madhusudana and B. K. Sadashiva, *Mol. Cryst. Liq. Cryst.*, 2001, **365**, 755.
- 9 B. K. Sadashiva, R. Amaranatha Reddy, R. Pratibha and N. V. Madhusudana, *Chem. Commun.*, 2001, 2140.
- 10 B. K. Sadashiva, R. Amaranatha Reddy, R. Pratibha and N. V. Madhusudana, *J. Mater. Chem.*, 2002, **12**, 943.

- 11 M. Prehm, X. H. Cheng, S. Diele, M. K. Das and C. Tschierske, *J. Am. Chem. Soc.*, 2002, **124**, 12072.
- 12 E. Eremin, S. Diele, G. Pelzl, H. Nadasi, W. Weissflog, J. Salfetnikova and H. Kresse, *Phys. Rev. E: Stat. Phys., Plasmas, Fluids, Relat. Interdiscip.*, 2001, **64**, 51707.
- 13 G. W. Gray, C. Hogg and D. Lacey, *Mol. Cryst. Liq. Cryst.*, 1981, **67**, 1.
- 14 N. Kasthuraiah, B. K. Sadashiva, S. Krishnaprasad and G. G. Nair, *Liq. Cryst.*, 1998, **24**, 639.
- 15 M. W. Schroder, S. Diele, N. Pancenko, W. Weissflog and G. Pelzl, *J. Mater. Chem.*, 2002, **12**, 1331.
- 16 H. R. Brand and H. Pleiner, *Makromol. Chem. Rapid Commun.*, 1991, **12**, 539.
- 17 Y. Takanishi, H. Takezoe, A. Fukuda, H. Komura and J. Watanabe, *J. Mater. Chem.*, 1992, **2**, 71.
- 18 Y. Takanishi, H. Takezoe, A. Fukuda and J. Watanabe, *Phys. Rev. B*, 1992, **45**, 7684.
- 19 X. F. Han, S. T. Wang, A. Cady, Z. Q. Liu, B. K. Sadashiva, R. Amaranatha Reddy and C. C. Huang, presented at the 9th International Ferroelectric Liquid Crystal Conference, Dublin, Ireland, August 24–29, 2003, poster 93.